

# The position of the spinal cord relative to the vertebrae in adolescent idiopathic scoliosis

Masashi Miyazaki, MD, PhD<sup>a,\*</sup>, Toshinobu Ishihara, MD, PhD<sup>a</sup>, Tetsutaro Abe, MD<sup>a</sup>, Shozo Kanezaki, MD<sup>a</sup>, Naoki Notani, MD<sup>a</sup>, Masashi Kataoka, MD, PhD<sup>b</sup>, Hiroshi Tsumura, MD, PhD<sup>a</sup>

## Abstract

We aimed to clarify the position of the spinal cord relative to the vertebra in patients with Lenke type 1 adolescent idiopathic scoliosis (AIS). In all, 35 patients with Lenke type 1 AIS who underwent posterior spinal fusion using a pedicle screw construct and preoperative computed tomography (CT) after myelography were recruited. The following radiological parameters were measured on preoperative CT myelography: spinal cord–vertebral (SV) angle, entry–spinal cord distance (ESD), ESD-X, ESD-Y, spinal cord–pedicle (SP) angle, and rotation angle (RASag). The SV and SP angles were the smallest at T9 level, followed by T8 and T7 levels, and tended to increase cranially and caudally. The ESD was the shortest at T9 level, followed by T8 and T10 levels. The ESD-X was the smallest at T9 level, followed by T8 level, while the ESD-Y was the smallest at T10 level, followed by T9 and T8 levels. Mean RASag increased from T4 to T9 levels and decreased from T9 to T12 levels. The ESD was significantly negatively correlated to RASag. Among all apical vertebrae, the SV and SP angles were negatively correlated to Cobb angle. The RASag was positively correlated while the ESD was negatively correlated to the Cobb angle. The spinal cord is close to the vertebrae in the apical vertebral region and far from the vertebrae at the upper and lower thoracic vertebral levels in AIS. Therefore, the potential risk of spinal cord injury by pedicle screw is the highest in the apical vertebral region.

**Abbreviations:** AIS = adolescent idiopathic scoliosis, CT = computed tomography, ESD = entry–spinal cord distance, RASag = rotation angle, SP = spinal cord–pedicle, SV = spinal cord–vertebral.

**Keywords:** adolescent idiopathic scoliosis, apical vertebra, computed tomography, myelography, pedicle screw, scoliosis, spinal cord injury

## 1. Introduction

Adolescent idiopathic scoliosis (AIS) is a complex spine deformity with different grades of spine involvement in the frontal, sagittal, and axial planes. Posterior spinal correction and fusion with

segmental pedicle screw instrumentation is the mainstay of surgery for AIS, allowing segmental instrumentation in multiple vertebrae across a multilevel fusion area and providing strong pullout strength and desired deformity correction.<sup>[1–3]</sup> Despite its advantages, its efficacy remains controversial when applied at the thoracic level, owing to relatively small pedicle dimensions.<sup>[4]</sup> Screw misplacement may reduce the pullout strength or lead to severe complications involving the nearby visceral, vascular, and neurologic structures.<sup>[5–7]</sup>

The incidence of screw misplacement increased up to 43%<sup>[8,9]</sup> when all screws were postoperatively evaluated by computed tomography (CT). Thoracic pedicle screw fixation is potentially risky because of little space between the spinal cord and medial wall of pedicle in the concave side of nearby apex vertebrae. The incidence of screw-related neurologic complications ranges from 0% to 0.9%<sup>[8,9]</sup> during the treatment of spinal deformities with thoracic pedicle screws. Mac-Thiong et al<sup>[7]</sup> reported 9 cases of total pedicle screw misplacement relative to the spinal canal during posterior surgery for AIS; furthermore, the incidence of spinal canal intrusion was 21% to 61% in this study. Sarlak et al<sup>[10]</sup> also reported that the rate of medial misplaced pedicle screws was 10.8% in a study of 1797 screws in 148 patients with scoliosis. They suggested that the acceptability of medial pedicle breach might change at each level with different canal width and different amount of cord shift.

Although various anatomic studies on the unique characteristics of thoracic vertebrae in AIS have been previously conducted,<sup>[4,11,12]</sup> few studies have investigated the position of the spinal cord in spinal canal in AIS. When evaluating the spinal cord relative to vertebrae in AIS, it may be more informative to

Editor: Shogo Hayashi.

All procedures performed in studies involving human participants were in accordance with the ethical standards of the institutional and/or national research committee and with the 1964 Helsinki declaration and its later amendments or comparable ethical standards.

Informed consent was obtained from all individual participants included in the study.

The authors declare that they have no conflict of interest.

<sup>a</sup>Department of Orthopaedic Surgery, Faculty of Medicine, <sup>b</sup>Physical Therapy Course of Study, Faculty of Welfare and Health Sciences, Oita University, Oita, Japan.

\*Correspondence: Masashi Miyazaki, Department of Orthopaedic Surgery, Faculty of Medicine, Oita University, 1-1 Idaigaoka, Hasama-machi, Yufu-shi, Oita 879-5593, Japan (e-mail: masashim@oita-u.ac.jp).

Copyright © 2019 the Author(s). Published by Wolters Kluwer Health, Inc. This is an open access article distributed under the terms of the Creative Commons Attribution-Non Commercial License 4.0 (CCBY-NC), where it is permissible to download, share, remix, transform, and buildup the work provided it is properly cited. The work cannot be used commercially without permission from the journal.

How to cite this article: Miyazaki M, Ishihara T, Abe T, Kanezaki S, Notani N, Kataoka M, Tsumura H. The position of the spinal cord relative to the vertebrae in adolescent idiopathic scoliosis. *Medicine* 2019;98:47(e18057).

Received: 9 July 2019 / Received in final form: 18 September 2019 / Accepted: 23 October 2019

<http://dx.doi.org/10.1097/MD.00000000000018057>

select cases with a similar spine curve. Therefore, the purpose of the present study was to investigate the relative position of the spinal cord in the spinal canal in Lenke type 1 AIS before surgery.

## 2. Materials and methods

### 2.1. Patient demographic data

This was a retrospective study using prospectively collected data performed in a single academic teaching institution. This study included 35 patients with adolescent right thoracic idiopathic scoliosis classified as Lenke type 1 according to the Lenke classification.<sup>[13]</sup> The patients underwent pedicle screw fixation between 2011 and 2019. The following criteria were applied for patient selection:

1. AIS classified as Lenke type 1 and
2. available preoperative radiographs and CT myelography images.

Exclusion criteria were

1. proven or suspected congenital, muscular, neurologic, or hormonal causes of scoliosis and
2. clinical history of any condition that may affect vertebral growth (e.g., cancer history, vertebral abnormalities, muscular abnormalities, or neurologic conditions).

Posteroanterior standing preoperative radiographs of the spine were reviewed to determine the Cobb angle of thoracic curves, the

**Table 1**

#### Patient demographic data.

Parameters	Mean $\pm$ SD/n (%)
Age (yrs)	15.6 $\pm$ 1.8
Gender	
Male	4 (11.4)
Female	31 (88.6)
Height (cm)	157.9 $\pm$ 6.2
Weight (kg)	49.6 $\pm$ 6.9
Cobb angle (°)	56.7 $\pm$ 12.6
Apical vertebrae	
T7	3 (8.6)
T8	9 (25.7)
T9	13 (37.1)
T10	7 (20.0)
T11	3 (8.6)
Lumber modifier	
1A	18 (51.4)
1B	13 (37.1)
1C	4 (11.4)

apex vertebra of the curves, and lumbar modifier. Additionally, CT scans were routinely obtained after myelography. All patients who underwent surgery during that period also underwent CT myelography, which were available for analysis. Applying these criteria, 35 (4 male and 31 female) patients with a mean age of

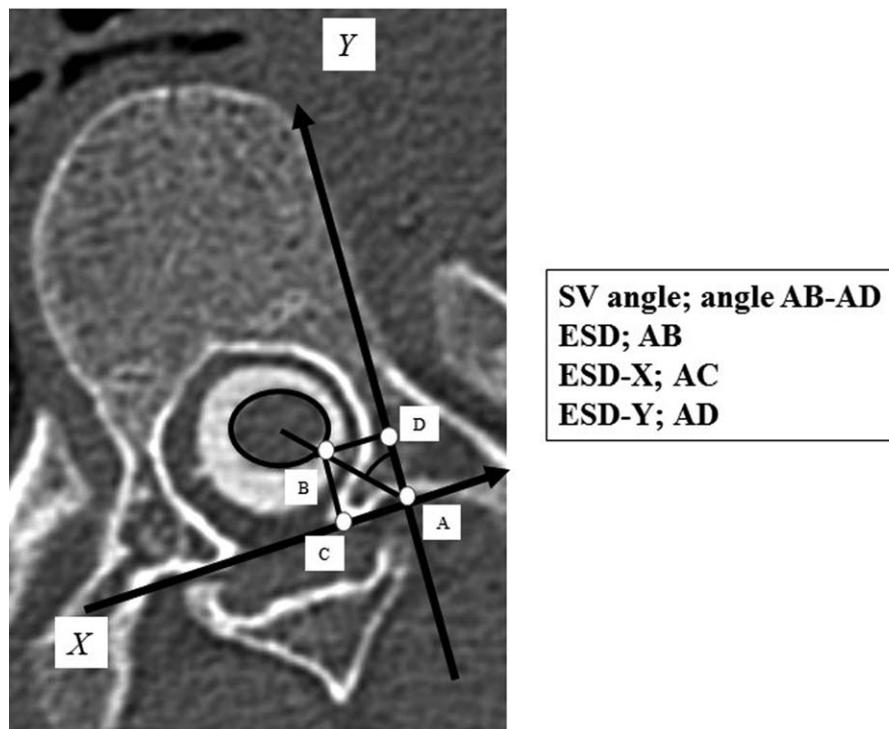


**Figure 1.** Illustration of a thoracic vertebra, showing the Spinal cord–Vertebral angle (SV angle), Entry–Spinal cord distance (ESD), ESD-X, and ESD-Y. We selected the point where the left pedicle axial line intersected the base of the left transverse process (point A). A line connecting the middle points of both bases of the superior facets was defined as the pedicular line (X-axis). The Y-axis perpendicular to the X-axis was drawn ventrally from the origin. The angle formed by the Y-axis and a line connecting the origin and the center of the spinal cord was defined as the left Spinal cord–Vertebral angle (SV angle; angle AB-AD), the length of a line connecting the origin and the edge of the spinal cord was defined as the left Entry–Spinal cord distance (ESD; AB). Moreover, we divided the left ESD distance into the X- and Y-units. The X-unit was the rectangular component of the left ESD distance on the X-axis (ESD-X; AC) and the Y-unit was the rectangular component of the left ESD distance on the Y-axis (ESD-Y; AD).

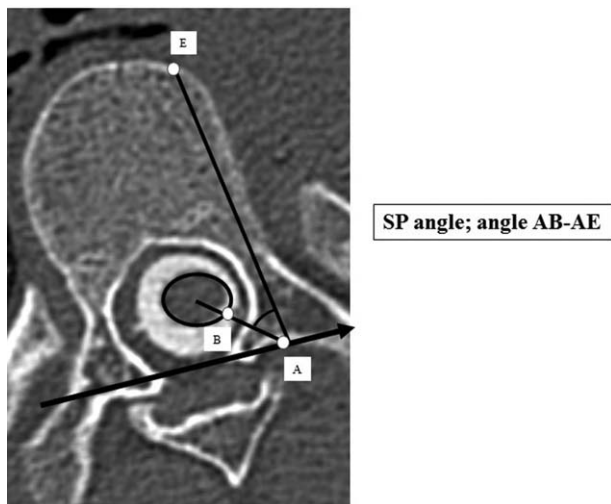


**Figure 2.** Illustration of a thoracic vertebra, showing the Spinal cord–Pedicle angle (SP angle). The angle formed by the left pedicle axial line and a line connecting the origin and the center of the spinal cord was defined as the left Spinal cord–Pedicle angle (SP angle; angle AB-AE).

15.6 ± 1.8 years (range, 12–19 years) with Lenke type 1 AIS (1A: 18 patients, 1B: 13 patients, and 1C: 4 patients) were included. The mean Cobb angle of the main curve was 56.7° ± 12.6° (range, 45°–103°). The apex vertebrae ranged from T7 to T11, with T9 being the most common (13 patients, 37.1%), followed by T8 (9 patients, 25.7%), T10 (7 patients, 20.0%), T11 (3 patients, 8.6%), and T7 (3 patients, 8.6%). The mean height of the patients was 157.9 ± 6.2 cm (range, 145–173 cm), and the mean weight of the patients was 49.6 ± 6.9 kg (range, 31–74 kg) (Table 1).

## 2.2. Scanning protocol

The patients were placed in the prone position. After myelography, CT scans were obtained using a multislice scanner (Toshiba Aquilion 16, Toshiba Medical, Tochigi, Japan). Image data were obtained in 0.5-mm slices from the level of the occiput to S1. Each CT scan was opened with synchronized axial, coronal, and sagittal displays. The image contrast levels were standardized to enable clear soft tissue and bone demarcation at the level of each vertebra. For the measurement, the local axial viewing plane was adjusted to be parallel to the superior and inferior endplates of the vertebrae. When the superior and inferior endplate planes were not parallel owing to vertebral wedging, an orientation approximately halfway between (i.e., bisecting) the 2 endplate inclinations was selected. Axial images were selected from T4 to T12 vertebrae and 315 images were analyzed.

The measurement was performed by using Picture Archiving and Communication System software. A new coordinate system was defined. The point where the left pedicle axial line intersected the base of the left transverse process (point A) was selected as the origin of this coordinate system because this point is mostly chosen for pedicle screw insertion during practical surgery. A line connecting the middle points of both bases of the superior facets was defined as the pedicular line (X-axis). The Y-axis perpendicular to the X-axis was drawn ventrally from the origin. The angle formed by the Y-axis and a line connecting the origin

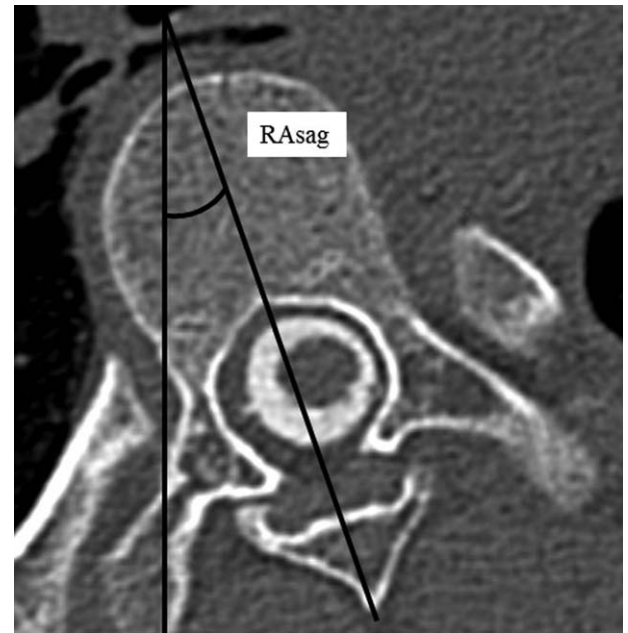


**Figure 3.** Illustration of a thoracic vertebra, showing the angle of rotation (RASag). RASag was measured by using the angle between a line connecting the junction of the laminae to the dorsal central aspect of the vertebral foramen and a line drawn through the middle of the vertebral body in the sagittal plane.

and the center of the spinal cord was defined as the left spinal cord–vertebral angle (SV angle; angle AB-AD), and the length of a line connecting the origin and the edge of the spinal cord as the left entry–spinal cord distance (ESD; AB). Moreover, we divided the left ESD distance into the X- and Y-units. The X-unit was the rectangular component of the left ESD distance to the X-axis (ESD-X; AC), and the Y-unit was the same to the Y-axis (ESD-Y; AD) (Fig. 1). The angle formed by the left pedicle axial line and a line connecting the origin and the center of the spinal cord was defined as the left spinal cord–pedicle angle (SP angle; angle AB-AE) (Fig. 2).

Rotation angle (RASag) of the vertebra was measured using the angle between a line connecting the junction of the laminae to the dorsal central aspect of the vertebral foramen and a line drawn through the middle of the vertebral body in the sagittal plane<sup>[14]</sup> (Fig. 3).

Two independent observers (T.I. and T.A.) measured each parameter in consensus (intra- and inter-observer agreement was good to excellent for each parameter; kappa > 0.70).

The apical vertebra of each patient was selected for sub-analysis and the correlation between the parameters at the apical vertebra and main thoracic Cobb angle magnitude was analyzed.

## 2.3. Statistical analysis

The variables measured in the study are expressed as mean ± SD. Wilcoxon signed-rank test was used to evaluate differences between the measured data. Pearson correlation coefficient was used to evaluate the association between the parameters. Differences were considered statistically significant when *P* value was < .05. All statistical analyses were performed using SPSS (version 13; SPSS, Chicago, IL).

**Table 2**  
**SV angle and SP angle.**

Level	SV angle (°)		SP angle (°)	
T4	51.7±5.6	<i>P</i> <.001**	46.8±6.2	<i>P</i> <.001**
T5	45.6±7.0	<i>P</i> <.001**	40.6±7.2	<i>P</i> <.001**
T6	42.5±7.8	<i>P</i> =.026*	38.0±8.1	<i>P</i> =.043*
T7	40.7±7.0	<i>P</i> =.194	36.4±6.8	<i>P</i> =.227
T8	39.7±5.6	<i>P</i> =.435	35.4±4.4	<i>P</i> =.519
T9	38.5±7.9	N/A	34.6±5.6	N/A
T10	45.3±10.8	<i>P</i> <.001**	40.3±12.2	<i>P</i> =.005**
T11	51.5±7.6	<i>P</i> <.001**	46.1±9.4	<i>P</i> <.001**
T12	54.1±8.9	<i>P</i> <.001**	47.8±8.2	<i>P</i> <.001**

*P*, statistical difference between each figures and minimum SV angle (T9) or SP angle (T9).

\* *P*<.05.

\*\* *P*<.01.

### 3. Results

#### 3.1. SV and SP angles

The relative position of the spinal cord to the vertebrae changed dramatically at the thoracic level of the spine. The SV angle was smallest at the T9 level, followed by T8 and T7 levels, and tended to increase cranially and caudally. The SV angle at T9 level was significantly smaller than that at T4, T5, T6, and T10–T12 levels. Additionally, the SP angle was smallest at the T9 level followed by T8 and T7 levels, and tended to increase cranially and caudally. The SP angle at T9 level was significantly smaller than those of T4, T5, T6, and T10–T12 levels (Table 2).

#### 3.2. ESD, ESD-X, and ESD-Y

The ESD was shortest at the T9 level followed by T8 and T10 levels, and tended to increase cranially and caudally (Table 3, Fig. 4). The ESD at T9 level was significantly shorter than those at T4, T5, T6, T7, and T11–T12 levels. Additionally, the ESD-X was smallest at the T9 level, followed by T8, while ESD-Y was smallest at the T10 level, followed by T9 and T8 levels. Both parameters tended to increase cranially and caudally. The ESD-X at T9 level was significantly shorter than those at T4, T5, T6, and T10–T12 levels, while the ESD-Y at T10 level was significantly shorter than those at T4, T5, T6, T7, and T11–T12 levels (Table 3, Fig. 5).

#### 3.3. Rotation angle of the vertebra (RASag)

The mean RASag increased from T4 to T9 and decreased from T9 to T12 (Table 4). The RASag was the largest at T9 level, followed by T8, T7, and T10 levels, and tended to decrease cranially and caudally (Table 4). The RASag at T9 level was significantly larger than that at T4, T5, T6, and T11–T12 levels.

#### 3.4. Correlation of ESD and RASag

ESD was significantly negatively correlated to RASag ( $r=-0.267$ ,  $P<.001$ ) (Fig. 6).

#### 3.5. Apical vertebral parameters and correlation with Cobb angle

The mean SV angle ( $r=-0.348$ ,  $P=.020$ ), SP angle ( $r=-0.443$ ,  $P=.004$ ), ESD ( $r=-0.377$ ,  $P=.030$ ), ESD-X ( $r=-0.387$ ,  $P=.031$ ), and ESD-Y ( $r=-0.330$ ,  $P=.026$ ) showed a significant negative correlation with Cobb angle, while RASag ( $r=0.531$ ,  $P=.001$ ) showed a significant positive correlation with the Cobb angle (Table 5).

### 4. Discussion

Pedicle screw fixation had been widely accepted as the preferred spinal implant instrumentation for corrective surgery of spine

**Table 3**  
**ESD, ESD-X and ESD-Y.**

Level	ESD (mm)		ESD-X (mm)		ESD-Y (mm)	
T4	14.1±2.3	<i>P</i> <.001**	10.8±2.2	<i>P</i> <.001**	9.0±1.6	<i>P</i> <.001**
T5	13.8±2.2	<i>P</i> <.001**	9.6±2.3	<i>P</i> <.001**	10.0±1.6	<i>P</i> <.001**
T6	11.8±2.5	<i>P</i> <.001**	7.7±2.2	<i>P</i> <.001**	9.0±2.1	<i>P</i> <.001**
T7	9.8±2.3	<i>P</i> <.001**	6.2±1.8	<i>P</i> =.002**	7.6±1.8	<i>P</i> <.001**
T8	8.3±1.8	<i>P</i> =.235	5.4±1.3	<i>P</i> =.249	6.7±1.6	<i>P</i> =.071
T9	7.9±1.8	N/A	5.0±1.6	N/A	6.2±1.6	<i>P</i> =.277
T10	8.3±2.2	<i>P</i> =.210	6.1±1.7	<i>P</i> <.001**	5.8±2.3	N/A
T11	10.8±2.7	<i>P</i> <.001**	8.5±2.1	<i>P</i> <.001**	6.6±2.5	<i>P</i> =.043*
T12	14.0±3.6	<i>P</i> <.001**	11.0±3.3	<i>P</i> <.001**	8.6±2.6	<i>P</i> <.001**

*P*, statistical difference between each figures and minimum ESD (T9) or ESD-X (T9) or ESD-Y (T10).

\* *P*<.05.

\*\* *P*<.01.

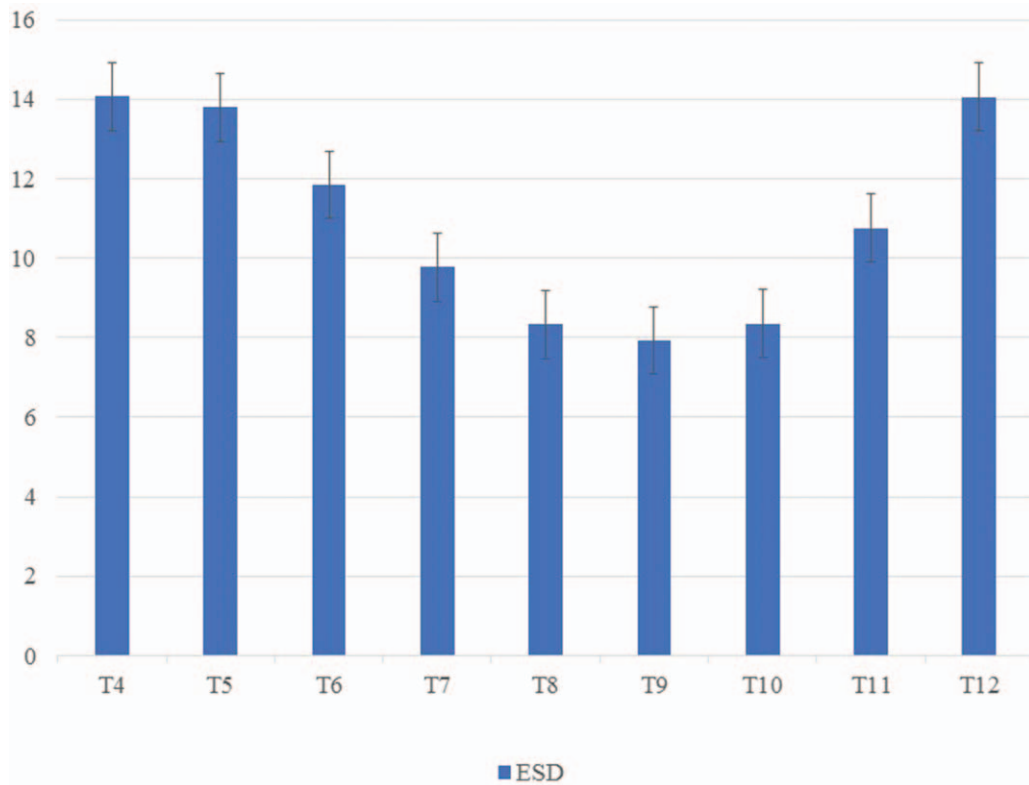


**Figure 4.** Entry–Spinal cord distance (ESD). The graph shows ESD at each anatomic vertebral level. The ESD was shortest at the T9 level followed by T8 and T10 levels, and tended to increase cranially and caudally. The ESD at T9 level was significantly shorter than those at T4, T5, T6, T7, and T11–T12 levels.

**Table 4**  
The angle of rotation (RASag).

Level	RASag (°)	P-value
T4	17.9 ± 3.2	P < .001**
T5	18.6 ± 3.7	P < .001**
T6	21.5 ± 5.6	P = .010*
T7	24.1 ± 5.8	P = .348
T8	24.7 ± 4.0	P = .698
T9	25.1 ± 6.4	N/A
T10	23.9 ± 5.2	P = .337
T11	21.3 ± 4.0	P = .002**
T12	20.3 ± 4.1	P < .001**

P, statistical difference between each figures and maximum RASag (T9).  
\* P < .05.  
\*\* P < .01.

deformities. However, a recent study performed on 140 AIS patients with 2020 pedicle screws implanted showed a perforation rate of 20.3%, with only 2.2% critical perforations.<sup>[15]</sup> Dural tears, aortic injury, neural injury, and lung complications such as pleural effusion and pneumothorax have been reported as the complications of pedicle screw insertion.<sup>[5]</sup> Among these complications, iatrogenic spinal cord injury is one of the most severe complications of scoliosis correction. Although many studies have addressed the vertebral morphology of AIS,<sup>[4,11,12,16–18]</sup> the position of the spinal cord in the spinal canal in AIS has not been quantified sufficiently. The placement of pedicle screws in the thoracic spine for the treatment of pediatric spinal deformity had been reported to be safe despite the high rate of malpositioned screws. However, neurologic complications were encountered and reported. Hicks et al<sup>[6]</sup> reported 7 pedicle

**Table 5**  
Apical vertebral parameters and its correlation with Cobb angle magnitude.

SV angle (°)			SP angle (°)			RASag (°)		
Mean ± SD	r	P	Mean ± SD	r	P	Mean ± SD	r	P
36.3 ± 8.0	-0.348	.020*	32.1 ± 5.3	-0.443	.004**	26.6 ± 5.5	0.531	.001**
ESD (mm)			ESD-X (mm)			ESD-Y (mm)		
Mean ± SD	r	P	Mean ± SD	r	P	Mean ± SD	r	P
7.5 ± 1.6	-0.377	.030*	4.5 ± 1.6	-0.387	.031*	5.8 ± 1.3	-0.330	.026*

\* P < .05.  
\*\* P < .01.

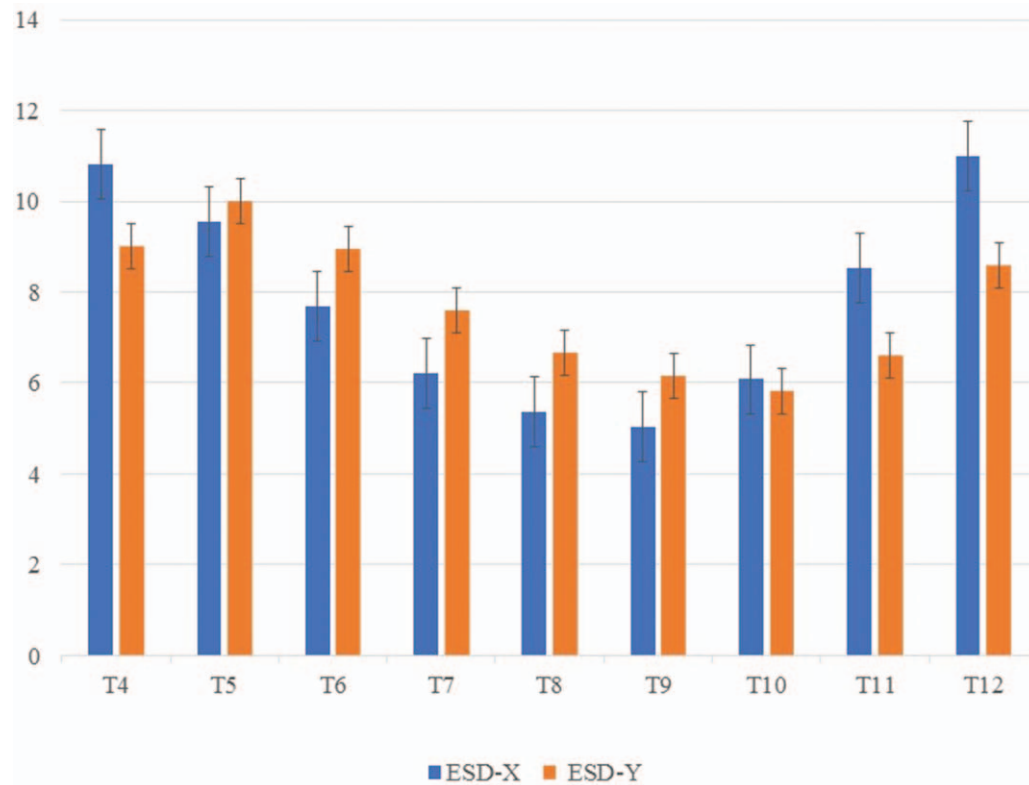


**Figure 5.** ESD-X, ESD-Y. The graph shows ESD-X and ESD-Y at each anatomic vertebral level. ESD-X was smallest at the T9 level, followed by T8 level, while ESD-Y was smallest at the T10 level, followed by T9 and T8 levels. Both parameters tended to increase cranially and caudally. The ESD-X at T9 level was significantly shorter than those of T4, T5, T6, and T10–T12 levels, and the ESD-Y at T10 level was significantly shorter than those of T4, T5, T6, T7, and T11–T12 levels.

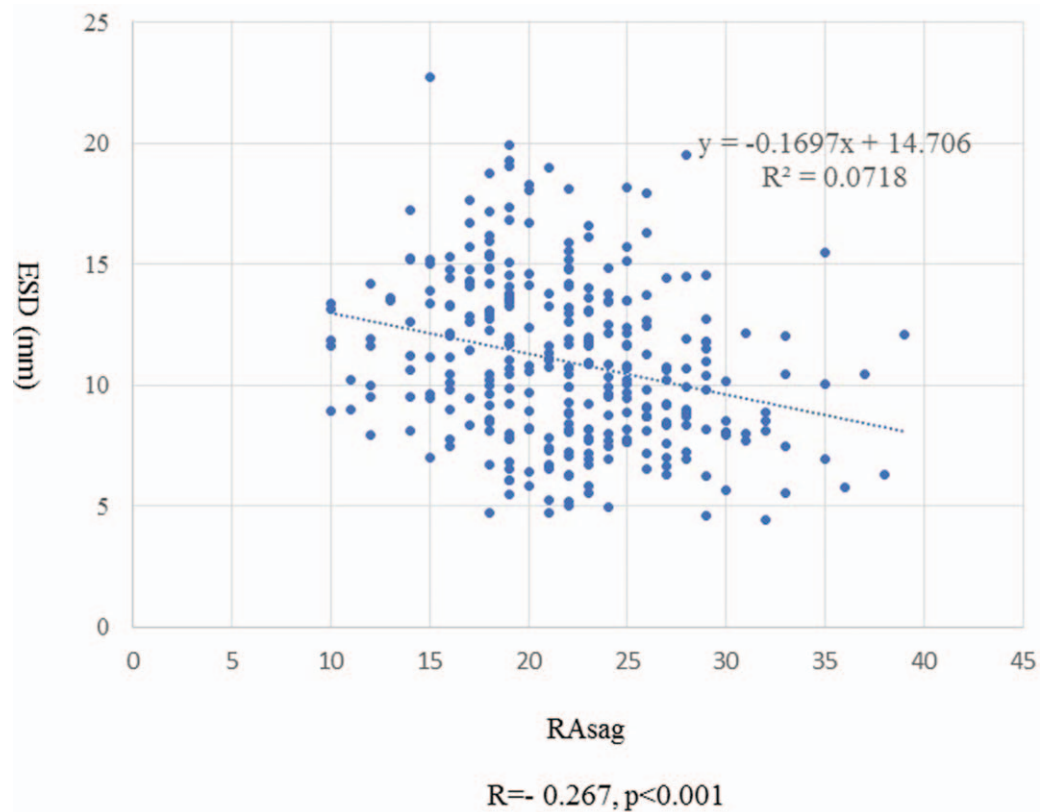


**Figure 6.** Correlation of ESD and RAsag. ESD was significantly negatively correlated to RAsag ( $r = -0.267, P < .001$ ).

screw complications over a 17-year period of AIS treatment, including thoracic pain with radiculopathy, somatosensory-evoked potentials disappearance after screw insertion, Brown-Sequard syndrome, paraplegia, and catastrophic neurologic events. Furthermore, 3 studies reported dural leaks during screw placement.<sup>[5,9,19]</sup>

Pedicle screws are often applied at the apex because of the better correction strength. However, few investigations have reported on the safety of this procedure and the relative position of the spinal cord to pedicle. Smorgick et al.<sup>[20]</sup> retrospectively reviewed magnetic resonance imaging (MRI) findings of 45 patients with AIS and showed that spinal cord in AIS tended to follow the appearance of the curve, being tethered on the concave side and the immediate proximity of the spinal cord to the pedicle around the apex area. Wang et al.<sup>[21]</sup> also reviewed MRI findings of 33 patients with AIS and investigated the relative position of the spinal cord in the spinal canal. They reported that the average distance from the spinal cord to the medial wall of pedicle at the concave side was significantly lower than that at the convex side. Although the result and conclusion were same to the present study, previous studies<sup>[20,21]</sup> were based on MRI. MRI is a less invasive tool that can visualize soft tissue morphometry better than CT myelography. The disadvantages of MRI are the limitation of the number of image slices. Image data of CT myelography were obtained in 0.5-mm slices in the present study. It is a better tool for visualizing osseous vertebral morphology and the spinal cord in detail. Furthermore, a multiplanar reconstruction view of CT myelography can provide accurate data. Therefore, the present study was performed using CT myelography.

In the present study, we investigated the position of the spinal cord relative to the position of pedicle screw insertion point. The SP angle was smallest at the apex vertebra and tended to increase cranially and caudally. The ESD was also shortest at the apex vertebra and tended to increase cranially and caudally. Therefore, the potential risk of the spinal cord injury by pedicle screw is highest at the apical vertebral region. Sarwahi et al.<sup>[22]</sup> investigated the abnormal pedicles in spines with AIS and in normal cases. They found a significantly higher prevalence of abnormal pedicles in patients with AIS, and most of the abnormal pedicles were in the thoracic spine on the concave side and in the periapical and apical regions. This risk was further increased because of slimmer, more distorted, more sclerotic, and shorter pedicles in thoracic scoliosis.<sup>[23]</sup>

The present study also showed the mean RAsag was largest at the apex vertebra (T9) and tended to decrease cranially and caudally (Table 4), and the ESD was significantly correlated RAsag (Fig. 6). It indicates that the rotational deformity is largest at the apex vertebral region and support the conclusion that the potential risk of spinal cord injury by a pedicle screw increases around the apex vertebral region. Other anchoring methods may be selected when preoperative evaluation reveals narrow pedicles.<sup>[24]</sup>

The strength of the present study comparing previous studies<sup>[20,21]</sup> was to analyze the relationship between apical vertebra parameters and main thoracic Cobb angle magnitude. The mean SV and SP angles were significantly negative correlated to Cobb angle. The mean RAsag was significantly positive correlated to Cobb angle. The mean ESD, ESD-X, ESD-Y were significantly negative correlated to Cobb angle (Table 5). It indicated that the rotational deformity is larger at the apex vertebra in patients with larger Cobb angle, and the potential risk of the spinal cord injury

by pedicle screw is more increased at the apex vertebra in patients with larger thoracic Cobb angle.

There are still limitations in the present study. It would have been ideal if we could increase the sample of patients, repeat the same measurements in other patients with Lenke type 1 AIS, and observe if there are differences of these parameters among different Lenke curve types.

## 5. Conclusion

Our study showed the relative position of the spinal cord in the spinal canal in patients with Lenke type 1 AIS. The spinal cord was close to the vertebrae at the apical vertebral region and far away from the vertebrae at the upper and lower thoracic vertebral level. Pedicle screw placement in the concave side of the apex should be evaluated carefully before operation.

## Author contributions

**Conceptualization:** Masashi Miyazaki.

**Data curation:** Toshinobu Ishihara, Tetsutaro Abe.

**Investigation:** Naoki Notani.

**Supervision:** Masashi Kataoka, Hiroshi Tsumura.

**Visualization:** Shozo Kanezaki.

**Writing – original draft:** Masashi Miyazaki.

**Writing – review & editing:** Masashi Miyazaki.

## References

- [1] Hamill CL, Lenke LG, Bridwell KH, et al. The use of pedicle screw fixation to improve correction in the lumbar spine of patients with idiopathic scoliosis. Is it warranted? *Spine (Phila Pa 1976)* 1996; 21:1241–9.
- [2] Lehman RA Jr, Lenke LG, Keeler KA, et al. Operative treatment of adolescent idiopathic scoliosis with posterior pedicle screw-only constructs: minimum three-year follow-up of one hundred fourteen cases. *Spine (Phila Pa 1976)* 2008;33:1598–604.
- [3] Lenke LG, Kuklo TR, Ondra S, et al. Rationale behind the current state-of-the-art treatment of scoliosis (in the pedicle screw era). *Spine (Phila Pa 1976)* 2008;33:1051–4.
- [4] Vaccaro AR, Rizzolo SJ, Allardyce TJ, et al. Placement of pedicle screws in the thoracic spine. Part I: Morphometric analysis of the thoracic vertebrae. *J Bone Joint Surg Am* 1995;77:1193–9.
- [5] Di Silvestre M, Parisini P, Lolli F, et al. Complications of thoracic pedicle screws in scoliosis treatment. *Spine (Phila Pa 1976)* 2007; 32:1655–61.
- [6] Hicks JM, Singla A, Shen FH, et al. Complications of pedicle screw fixation in scoliosis surgery: a systematic review. *Spine (Phila Pa 1976)* 2010;35:E465–70.
- [7] Mac-Thiong JM, Parent S, Poitras B, et al. Neurological outcome and management of pedicle screws misplaced totally within the spinal canal. *Spine (Phila Pa 1976)* 2013;38:229–37.
- [8] Belmont PJ Jr, Klemme WR, Dhawan A, et al. In vivo accuracy of thoracic pedicle screws. *Spine (Phila Pa 1976)* 2001;26:2340–6.
- [9] Suk SI, Kim WJ, Lee SM, et al. Thoracic pedicle screw fixation in spinal deformities: are they really safe? *Spine (Phila Pa 1976)* 2001;26:2049–57.
- [10] Sarlak AY, Tosun B, Atmaca H, et al. Evaluation of thoracic pedicle screw placement in adolescent idiopathic scoliosis. *Eur Spine J* 2009;18:1892–7.
- [11] Liljenqvist UR, Allkemper T, Hackenberg L, et al. Analysis of vertebral morphology in idiopathic scoliosis with use of magnetic resonance imaging and multiplanar reconstruction. *J Bone Joint Surg Am* 2002;84-A:359–68.
- [12] Liljenqvist UR, Link TM, Halm HF. Morphometric analysis of thoracic and lumbar vertebrae in idiopathic scoliosis. *Spine (Phila Pa 1976)* 2000;25:1247–53.
- [13] Aaro S, Dahlborn M. The longitudinal axis rotation of the apical vertebra, the vertebral, spinal, and rib cage deformity in idiopathic

- scoliosis studied by computer tomography. *Spine (Phila Pa 1976)* 1981;6:567–72.
- [14] Lenke LG, Betz RR, Harms J, et al. Adolescent idiopathic scoliosis: a new classification to determine extent of spinal arthrodesis. *J Bone Joint Surg Am* 2001;83-A:1169–81.
- [15] Kwan MK, Chiu CK, Gani SM, et al. Accuracy and safety of pedicle screw placement in adolescent idiopathic scoliosis patients: a review of 2020 screws using computed tomography assessment. *Spine (Phila Pa 1976)* 2017;42:326–35.
- [16] Parent S, Labelle H, Skalli W, et al. Thoracic pedicle morphometry in vertebrae from scoliotic spines. *Spine (Phila Pa 1976)* 2004;29:239–48.
- [17] Abul-Kasim K, Ohlin A. Patients with adolescent idiopathic scoliosis of Lenke type-1 curve exhibit specific pedicle width pattern. *Eur Spine J* 2012;21:57–63.
- [18] Takeshita K, Maruyama T, Chikuda H, et al. Diameter, length, and direction of pedicle screws for scoliotic spine: analysis by multiplanar reconstruction of computed tomography. *Spine (Phila Pa 1976)* 2009;34:798–803.
- [19] Di Silvestre M, Bakaloudis G, Lolli F, et al. Posterior fusion only for thoracic adolescent idiopathic scoliosis of more than 80 degrees: pedicle screws versus hybrid instrumentation. *Eur Spine J* 2008;17:1336–49.
- [20] Smorgick Y, Settecerrri JJ, Baker KC, et al. Spinal cord position in adolescent idiopathic scoliosis. *J Pediatr Orthop* 2012;32:500–3.
- [21] Wang S, Qiu Y, Liu W, et al. The potential risk of spinal cord injury from pedicle screw at the apex of adolescent idiopathic thoracic scoliosis: magnetic resonance imaging evaluation. *BMC Musculoskelet Disord* 2015;16:310.
- [22] Sarwahi V, Sugarman EP, Wollowick AL, et al. Prevalence, distribution, and surgical relevance of abnormal pedicles in spines with adolescent idiopathic scoliosis vs. no deformity: a ct-based study. *J Bone Joint Surg Am* 2014;96:e92.
- [23] Cui G, Watanabe K, Hosogane N, et al. Morphologic evaluation of the thoracic vertebrae for safe free-hand pedicle screw placement in adolescent idiopathic scoliosis: a CT-based anatomical study. *Surg Radiol Anat* 2012;34:209–16.
- [24] Imagama S, Ito Z, Wakao N, et al. Posterior surgery for adolescent idiopathic scoliosis with pedicle screws and ultrahigh-molecular weight polyethylene tape: achieving the ideal thoracic kyphosis. *Clin Spine Surg* 2016;29:E376–83.